

Two-dimensional collective Hamiltonian for chiral and wobbling modes. II. Electromagnetic transitions

X. H. Wu (吴鑫辉),¹ Q. B. Chen (陈启博),² P. W. Zhao (赵鹏巍),¹ S. Q. Zhang (张双全),^{1,*} and J. Meng (孟杰)^{1,3,†}

¹State Key Laboratory of Nuclear Physics and Technology, School of Physics, Peking University, Beijing 100871, China

²Physik-Department, Technische Universität München, D-85747 Garching, Germany

³Yukawa Institute for Theoretical Physics, Kyoto University, Kyoto 606-8502, Japan



(Received 12 September 2018; published 3 December 2018)

We calculate the intraband electromagnetic transitions in the framework of a collective Hamiltonian for chiral and wobbling modes. By going beyond the mean-field approximation on the orientations of the rotational axis, the collective Hamiltonian provides descriptions of both the yrast band and collective excitation bands. For a system with one $h_{11/2}$ proton particle and one $h_{11/2}$ neutron hole coupled to a triaxial rotor ($\gamma = -30^\circ$), the intraband electromagnetic transitions given by the one-dimensional and two-dimensional collective Hamiltonian are compared with results obtained by using the tilted axis cranking approach and the particle rotor model. Compared with the tilted axis cranking approach, the electromagnetic transitions given by the collective Hamiltonian agree better with the transitions obtained by using the particle rotor model because quantum fluctuations are considered.

DOI: [10.1103/PhysRevC.98.064302](https://doi.org/10.1103/PhysRevC.98.064302)

I. INTRODUCTION

In the first paper of this series [1], the two-dimensional collective Hamiltonian method based on the tilted axis cranking (TAC) approach has been developed to describe the nuclear chirality [2] and wobbling motion [3], both of which provide direct evidence for the existence of nuclear triaxiality. The chirality in nuclear physics was first predicted by Frauendorf and Meng in 1997 [2], which stimulates lots of experimental efforts and more than 60 candidate chiral bands reported in the $A \sim 80, 100, 130$, and 190 mass regions. For recent reviews and detailed data tables, see Refs. [4–10]. The wobbling motion was originally suggested by Bohr and Mottelson in the 1970s [3] and has been observed in the $A \sim 160$ [11–16], 130 [17,18], and 100 [19,20] mass regions.

Theoretically, the nuclear chirality and wobbling motion have been extensively investigated with the particle rotor model (PRM) [2,3,21–42] and the tilted axis cranking (TAC) approaches based on either the Woods–Saxon mean field [17,43] or more fundamental density-functional theories [44–48]. Other approaches include the boson expansion approaches [49–52], the pair truncated shell model [53], and the projected shell model [54–58]. The TAC approach, based on a mean-field approximation, provides a clear picture for the chirality and wobbling motion in terms of the orientation of the angular-momentum vector relative to the density distribution. To describe the chiral and wobbling excitations beyond the mean field, the random-phase approximation was developed on top of the TAC solutions [59–69]. Alternatively, the collective Hamiltonian based on the TAC solutions proves

to be very successful [1,70–72]. In particular, the collective Hamiltonian method is promising for unifying the description of both quantum tunneling and vibrations.

In previous works [1,70], the one- and two-dimensional collective Hamiltonian (1DCH and 2DCH) were constructed and applied to investigate the chirality of the system with one $h_{11/2}$ proton particle and one $h_{11/2}$ neutron hole coupled to a triaxial ($\gamma = -30^\circ$) rotor. It is found that the chiral symmetry is restored in the collective Hamiltonian solutions, which are in agreement with the energy spectra for chiral doublet bands given by the PRM [2]. Similar approaches have also been used in describing the wobbling motions in the simple, longitudinal, and transverse wobblers [71] and in the nucleus ^{135}Pr [72]. Moreover, more excitation modes appear in the framework of the 2DCH, since both the broken chiral and signature symmetries are restored [1].

Besides the energy spectra, the electromagnetic (EM) transition properties are important observables in identifying the nuclear chirality or wobbling motion. Based on the model with the configuration $\pi(1h_{11/2}) \otimes \nu(1h_{11/2})^{-1}$ and $\gamma = -30^\circ$, the criteria for ideal nuclear chirality are as follows [4,7,73]: (i) near degeneracy of doublet bands; (ii) spin independence of $S(I)$; (iii) similar spin alignments; (iv) $B(M1)$ values and the resulting $B(M1)/B(E2)$ ratios present odd-even staggering behavior; (v) doublet bands have similar intraband $M1$ and $E2$ transition strengths; and (vi) interband $E2$ transitions vanish in the high-spin region. For wobbling motion, one of the most important features is that the interband EM transitions with $\Delta I = 1$ between the wobbling bands are dominated by $E2$ rather than by $M1$ [3,11,33,35,69].

In this work, the collective Hamiltonian in previous works [1,70–72] is extended to calculate the intraband EM transition

*sqzhang@pku.edu.cn

†mengj@pku.edu.cn

probabilities and compared with those given by the TAC and PRM. The paper is organized as follows: In Sec. II, the frameworks of the 1DCH and 2DCH are briefly introduced, and the formulas for the intraband EM transition probabilities are given. The numerical details are given in Sec. III. In Sec. IV, the calculated results are presented and compared with the TAC and PRM. Finally, a summary is given in Sec. V.

II. THEORETICAL FRAMEWORK

A. Collective Hamiltonian

The collective Hamiltonian can be derived, for example, by the generator coordinate method (GCM) [74], the adiabatic time-dependent Hartree–Fock (ATDHF) method [74,75], or the adiabatic self-consistent collective coordinate (ASCC) method [76,77].

The orientations of the rotational axis in a triaxial nucleus can be parametrized by the polar and the azimuth angles (θ, φ) . These two angles are chosen as the collective coordinates to describe the chiral and wobbling modes in the collective Hamiltonian method. Based on the TAC approach, the collective Hamiltonian of the azimuth angle φ (1DCH) [70–72] and of both the polar and azimuth angles (θ, φ) (2DCH) [1] have been constructed. Here, for completeness, the frameworks of both the 1DCH and 2DCH are briefly given.

1. One-dimensional collective Hamiltonian

The 1DCH is written as [70–72]

$$\mathcal{H}(\varphi) = \frac{1}{2}B(\varphi)\dot{\varphi}^2 + \mathcal{V}(\varphi), \quad (1)$$

in which $\mathcal{V}(\varphi)$ is the collective potential and $B(\varphi)$ is the mass parameter. The collective potential is obtained by minimizing the total Routhian $E^i(\theta, \varphi)$ in the TAC with respect to θ for given φ , and the corresponding $B(\varphi)$ is calculated following Ref. [70].

From the general Pauli prescription [78], the quantal collective Hamiltonian reads

$$\hat{\mathcal{H}} = -\frac{\hbar^2}{2\sqrt{B(\varphi)}} \frac{\partial}{\partial \varphi} \frac{1}{\sqrt{B(\varphi)}} + \mathcal{V}(\varphi). \quad (2)$$

The corresponding eigenenergies E^i and the wave functions $\Psi^i(\varphi)$ can be obtained by diagonalizing the Hamiltonian (2) via the basis expansion method; see Ref. [70] for details. The collective Hamiltonian (2) is invariant under the transformation $\hat{P}_\varphi : \varphi \rightarrow -\varphi$ [70]. The eigenvalues of \hat{P}_φ are “+” or “−,” depending on whether the state is symmetric or antisymmetric with respect to the transformation. Therefore, the eigenstates can be divided into two

separate groups, i.e., $P_\varphi = +$ and $P_\varphi = -$ groups, and the eigenenergies of the two groups can be labeled as E^i_+ and E^i_- , respectively.

2. Two-dimensional collective Hamiltonian

The 2DCH is written as

$$\mathcal{H}(\theta, \varphi) = \frac{1}{2}B_{\theta\theta}\dot{\theta}^2 + \frac{1}{2}B_{\theta\varphi}\dot{\theta}\dot{\varphi} + \frac{1}{2}B_{\varphi\varphi}\dot{\varphi}^2 + \mathcal{V}(\theta, \varphi), \quad (3)$$

in which $\mathcal{V}(\theta, \varphi)$ is the collective potential, and $B_{\theta\theta}(\theta, \varphi)$, $B_{\theta\varphi}(\theta, \varphi)$, $B_{\varphi\theta}(\theta, \varphi)$, $B_{\varphi\varphi}(\theta, \varphi)$ are the mass parameters, which can be obtained from the TAC calculations [1].

From the general Pauli prescription [78], the quantal collective Hamiltonian reads

$$\hat{\mathcal{H}} = -\frac{\hbar^2}{2\sqrt{w}} \left[\frac{\partial}{\partial \varphi} \frac{B_{\theta\theta}}{\sqrt{w}} \frac{\partial}{\partial \varphi} - \frac{\partial}{\partial \varphi} \frac{B_{\varphi\theta}}{\sqrt{w}} \frac{\partial}{\partial \theta} - \frac{\partial}{\partial \theta} \frac{B_{\theta\varphi}}{\sqrt{w}} \frac{\partial}{\partial \varphi} + \frac{\partial}{\partial \theta} \frac{B_{\varphi\varphi}}{\sqrt{w}} \frac{\partial}{\partial \theta} \right] + \mathcal{V}(\theta, \varphi), \quad (4)$$

in which w is the determinant of the mass parameter tensor,

$$w = \det B = \begin{vmatrix} B_{\theta\theta} & B_{\theta\varphi} \\ B_{\varphi\theta} & B_{\varphi\varphi} \end{vmatrix}. \quad (5)$$

The eigenenergies E^i and the corresponding wave functions $\Psi^i(\theta, \varphi)$ can be obtained by diagonalizing the Hamiltonian (4) via the basis expansion method; see Ref. [1] for details. The collective Hamiltonian (4) is invariant under the transformation $\hat{P}_\theta : \theta \rightarrow \pi - \theta$ or $\hat{P}_\varphi : \varphi \rightarrow -\varphi$ [1]. The eigenvalues of \hat{P}_θ and \hat{P}_φ are “+” or “−,” depending on whether the state is symmetric or antisymmetric with respect to the transformations. Therefore, the eigenstates can be divided into four separate groups ($P_\theta P_\varphi$), i.e., the positive-positive (++) , positive-negative (+−) , negative-positive (−+) , and negative-negative (−−) groups, and the eigenenergies of the four groups can be labeled as E^i_{++} , E^i_{+-} , E^i_{-+} , and E^i_{--} , respectively.

B. Electromagnetic transitions

Because the tilted angles θ and φ are chosen as the collective coordinates in the collective Hamiltonian, the quantum fluctuations of the tilted angles are now considered in the frameworks of the 1DCH and 2DCH. Therefore, for EM transitions, it is natural to go beyond the semiclassical approximation in the TAC approach to include the quantum fluctuation effects.

In the TAC, the EM transition probabilities are calculated as the expectation values of the corresponding operators $M1$ and $E2$ semiclassically [2,79],

$$B_{\text{TAC}}^{M1}(\theta, \varphi) = \frac{3}{8\pi} \{ [-\mu_z \sin \theta_J + \cos \theta_J (\mu_x \cos \varphi_J + \mu_y \sin \varphi_J)]^2 + [\mu_y \cos \varphi_J - \mu_x \sin \varphi_J]^2 \}, \quad (6)$$

$$B_{\text{TAC}}^{E2(I \rightarrow I-2)}(\theta, \varphi) = \frac{15}{128\pi} \left\{ \left[Q_{20} \sin^2 \theta_J + \sqrt{\frac{2}{3}} Q_{22} (1 + \cos^2 \theta_J) \cos 2\varphi_J \right]^2 + \frac{8}{3} [Q_{22} \cos \theta_J \sin 2\varphi_J]^2 \right\}, \quad (7)$$

$$B_{\text{TAC}}^{E2(I \rightarrow I-1)}(\theta, \varphi) = \frac{5}{16\pi} \left\{ \left[\sin \theta_J \cos \theta_J \left(Q_{22} \cos 2\varphi_J - \sqrt{\frac{3}{2}} Q_{20} \right) \right]^2 + [\sin \theta_J \sin 2\varphi_J Q_{22}]^2 \right\}, \quad (8)$$

in which the intrinsic magnetic moments $\mu_i = \sum_{\tau=p,n} (g_\tau - g_R) \langle j_{i(\tau)} \rangle$ with the g factors g_τ (g_R) for valence nucleons (rotor) and the angular-momentum components $j_{i(\tau)}$ of valence nucleons on the i th axis, and the intrinsic electric-quadrupole tensors $Q_{20} = Q_0 \cos \gamma$ and $Q_{22} = Q_0 \sin \gamma / \sqrt{2}$ with the intrinsic electric-quadrupole moment Q_0 .

Note that the orientational angles (θ_J, φ_J) in Eqs. (6)–(8) describe the orientations of the angular momentum \mathbf{J} in the intrinsic frame and are in general different from the tilted cranking angles (θ, φ) in the TAC. For given tilted cranking angles (θ, φ) in the TAC, the components of \mathbf{J} are calculated by

$$J_k = \langle \hat{j}_k \rangle + \mathcal{J}_k \omega_k, \quad k = 1, 2, 3, \quad (9)$$

where the first term is from the valence particles and holes, and the second term from the rotor. The orientational angles (θ_J, φ_J) are defined as

$$\tan \theta_J = \frac{\sqrt{J_1^2 + J_2^2}}{J_3}, \quad \tan \varphi_J = \frac{J_2}{J_1}. \quad (10)$$

In the TAC, the self-consistent solution is obtained by minimizing the total Routhian, in which the tilted cranking angles (θ, φ) are the same as the orientational angles (θ_J, φ_J) . In such a case, the EM transitions are calculated with $(\theta_J, \varphi_J) = (\theta, \varphi)$, and the contributions from other orientations are neglected. The effects of the quantum fluctuations on EM transitions will be considered in the frameworks of the 1DCH and 2DCH.

1. Electromagnetic transitions in the one-dimensional collective Hamiltonian

In the 1DCH, the total Routhian $E^i(\theta, \varphi)$ is minimized with respect to θ for a given φ , and the collective wave function $\Psi^i(\varphi)$ represents the amplitude of the collective state i with azimuth angle φ . Hence, the EM transitions in Eqs. (6)–(8) only depend on azimuth angle φ . Therefore, the $M1$ and $E2$ transition probabilities in the 1DCH are

$$B_{\text{1DCH}}^{M1} = \int_{-\pi/2}^{\pi/2} d\varphi \sqrt{B(\varphi)} B_{\text{TAC}}^{M1}(\varphi) |\Psi(\varphi)|^2, \quad (11)$$

$$B_{\text{1DCH}}^{E2(I \rightarrow I-2)} = \int_{-\pi/2}^{\pi/2} d\varphi \sqrt{B(\varphi)} B_{\text{TAC}}^{E2(I \rightarrow I-2)}(\varphi) |\Psi(\varphi)|^2, \quad (12)$$

$$B_{\text{1DCH}}^{E2(I \rightarrow I-1)} = \int_{-\pi/2}^{\pi/2} d\varphi \sqrt{B(\varphi)} B_{\text{TAC}}^{E2(I \rightarrow I-1)}(\varphi) |\Psi(\varphi)|^2. \quad (13)$$

The angular momentum in the 1DCH is [70]

$$J_{\text{coll}}^{\text{1DCH}} = \int_{-\pi/2}^{\pi/2} d\varphi \sqrt{B(\varphi)} J_{\text{TAC}}(\varphi) |\Psi(\varphi)|^2. \quad (14)$$

Similarly, a quantal correction $I_{\text{coll}}^{\text{1DCH}} = J_{\text{coll}}^{\text{1DCH}} - 1/2$ [79] should be applied.

2. Electromagnetic transitions in the two-dimensional collective Hamiltonian

In the 2DCH, the collective wave function $\Psi^i(\theta, \varphi)$ represents the amplitude of the collective state i with polar and azimuth angles (θ, φ) .

Similar to the 1DCH, the $M1$ and $E2$ transition probabilities in the 2DCH are

$$B_{\text{2DCH}}^{M1} = \int_0^\pi d\theta \int_{-\pi/2}^{\pi/2} d\varphi \sqrt{w} B_{\text{TAC}}^{M1} \times (\theta, \varphi) |\Psi(\theta, \varphi)|^2, \quad (15)$$

$$B_{\text{2DCH}}^{E2(I \rightarrow I-2)} = \int_0^\pi d\theta \int_{-\pi/2}^{\pi/2} d\varphi \sqrt{w} B_{\text{TAC}}^{E2(I \rightarrow I-2)} \times (\theta, \varphi) |\Psi(\theta, \varphi)|^2, \quad (16)$$

$$B_{\text{2DCH}}^{E2(I \rightarrow I-1)} = \int_0^\pi d\theta \int_{-\pi/2}^{\pi/2} d\varphi \sqrt{w} B_{\text{TAC}}^{E2(I \rightarrow I-1)} \times (\theta, \varphi) |\Psi(\theta, \varphi)|^2, \quad (17)$$

and the angular momentum in the 2DCH is [1]

$$J_{\text{coll}}^{\text{2DCH}} = \int_0^\pi d\theta \int_{-\pi/2}^{\pi/2} d\varphi \sqrt{w} J_{\text{TAC}}(\theta, \varphi) |\Psi(\theta, \varphi)|^2. \quad (18)$$

A quantal correction $I_{\text{coll}}^{\text{2DCH}} = J_{\text{coll}}^{\text{2DCH}} - 1/2$ [79] is also applied.

III. NUMERICAL DETAILS

In the present calculations, a system with one $h_{11/2}$ proton particle and one $h_{11/2}$ neutron hole coupled to a triaxial rotor ($\gamma = -30^\circ$) is considered. The coupling coefficients in the single- j shell Hamiltonian are taken as $C_\pi = 0.25$ MeV for the proton particle and $C_\nu = -0.25$ MeV for the neutron hole. The moments of inertia for irrotational flow are adopted with $\mathcal{J}_0 = 40\hbar^2/\text{MeV}$. These numerical details are the same as those in Refs. [1,2,70]. In the calculations of the EM transition probabilities, the effective g factors are setting as $g_p - g_R = 1$ and $g_n - g_R = -1$, respectively, and the electric-quadrupole moment is taken as Q_0 . These assignments are the same in the calculations with the 1DCH, 2DCH, TAC, and PRM.

IV. RESULTS AND DISCUSSION

In Ref. [1], by taking the basis states under the periodic boundary condition and diagonalizing the collective Hamiltonian for given rotational frequencies, the collective energy levels and the wave functions obtained by the 2DCH

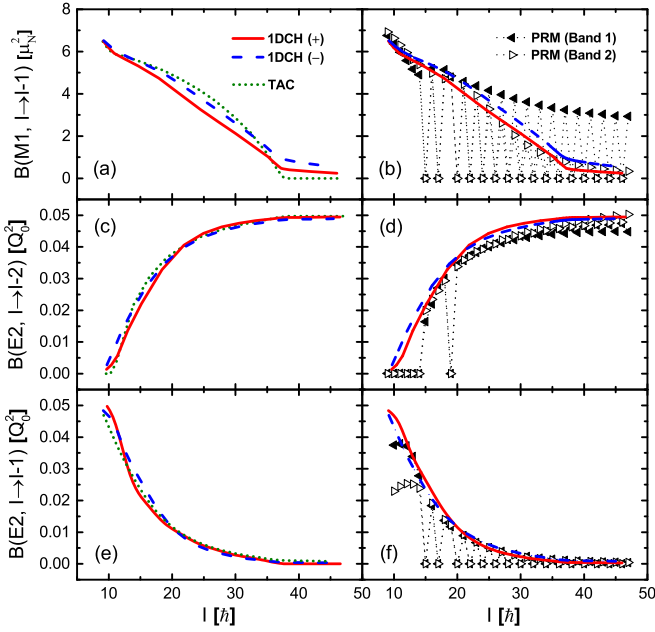


FIG. 1. The intraband $M1$ and $E2$ transition probabilities of the doublet bands obtained by the 1DCH in comparison with the TAC [(a), (c), (e)] and the PRM [(b), (d), (f)] as functions of spin.

have been compared with those obtained by the 1DCH. Meanwhile, the angular momenta and energy spectra calculated by the 2DCH have been compared with those by the TAC approach and the exact solutions of PRM. Here we follow the same 1DCH and 2DCH calculations in Ref. [1] and extend the discussion there to the intraband $M1$ and $E2$ transition probabilities.

A. One-dimensional collective Hamiltonian

In Fig. 1, the intraband $M1$ and $E2$ transition probabilities of the doublet bands, i.e., the lowest states in the groups (+) and (-), obtained by the 1DCH in comparison with those by the TAC and the PRM as functions of spin are given.

In Figs. 1(a), 1(c), and 1(e), it is found that the tendencies of the $M1$ and $E2$ transition probabilities of the yrast band (E_{+}^{\perp}) in the 1DCH agree well with those in the TAC. In Ref. [2], it was shown that the TAC could reproduce the intraband transition probabilities for the yrast band in the PRM. The description of the chiral and wobbling excitations is beyond the mean-field approximation in the TAC. The 1DCH takes the quantum fluctuation of the azimuth angle φ into account and thus provides the intraband EM transition probabilities of both the yrast band (E_{+}^{\perp}) and sideband (E_{-}^{\perp}). The obtained $M1$ and $E2$ transition probabilities for both bands are close to each other, as required by the chiral doublet bands or wobbling excitation bands.

In Fig. 1(a), the $B(M1)$ values in the TAC drop rapidly to zero around $I = 37\hbar$. This is because the values of both the polar and azimuth angles in the TAC become $\pi/2$ at this spin (see Figs. 2 and 4), which means that the nucleus rotates with the intermediate axis. According to Eq. (6), the $M1$ transitions vanish.

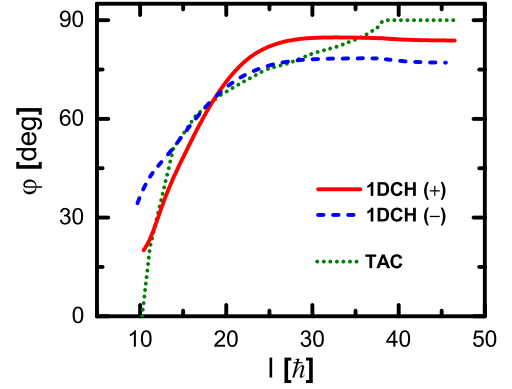


FIG. 2. The effective azimuth angles φ^{eff} of in the doublet bands obtained by the 1DCH as functions of spin in comparison with the azimuth angle φ by the TAC.

In contrast, the $B(M1)$ values in the 1DCH approach to zero smoothly. This can be understood from the effective azimuth angles φ^{eff} in the 1DCH defined as

$$\varphi_{\text{1DCH}}^{\text{eff}} = \int_{-\pi/2}^{\pi/2} d\varphi \sqrt{B(\varphi)} |\varphi| |\Psi(\varphi)|^2. \quad (19)$$

It is the expectation value of azimuth angle $|\varphi|$ including the quantum fluctuation effects of the orientational angles, and is displayed in Fig. 2.

Due to the quantum fluctuations, the orientation of angular momentum does not align with the intermediate axis at high spin but rather has a distribution. As a result, the effective azimuth angle φ^{eff} deviates from $\pi/2$, and the missing quantum effects in the TAC are resumed in the 1DCH. Therefore, the $B(M1)$ values in the 1DCH, although small, are nonvanishing at high spin.

In Figs. 1(b), 1(d), and 1(f), the intraband $M1$ and $E2$ transition probabilities in the 1DCH are compared with those in the PRM. For $B(E2, I \rightarrow I - 2)$ values, both results of the yrast and sidebands in the 1DCH agree well with those given by the PRM. For $B(M1)$ and $B(E2, I \rightarrow I - 1)$ values, however, there is a noticeable difference between the PRM and the 1DCH. The results in the PRM present strong odd-even staggering behavior, whereas those in the 1DCH do not. The staggering behavior of the EM transitions of chiral doublet bands in the PRM has been analyzed in Ref. [22]. In the 1DCH, the angular momentum is not a good quantum number. Therefore, the staggering behavior, which depends strongly on the quantized angular momentum, is not reproduced in the 1DCH. Similar arguments hold true for the TAC results where the staggering behavior cannot be reproduced, either. Nevertheless, it should be mentioned that the $B(M1)$ values in the PRM, regardless of the staggering behavior, are also not exactly zero at high spin, in accordance with the results from the 1DCH.

Staggering behavior is shown in the $B(M1)$ and $B(E2, I \rightarrow I - 1)$ values obtained from the PRM above $I = 15\hbar$. The underlying reason can be attributed to the selection rule, proposed in Ref. [22]. It is noted that the staggering feature is related to the ways in which one arranges the bands [80]. Since the bands in 1DCH or 2DCH are naturally

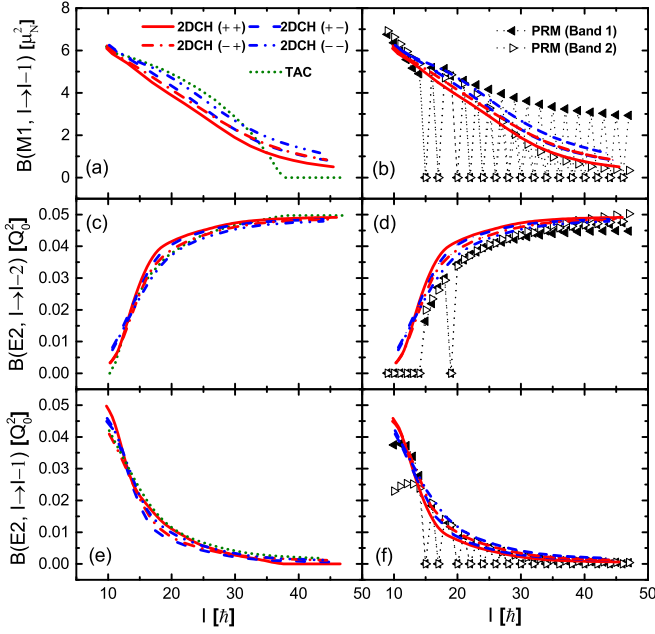


FIG. 3. The intraband $M1$ and $E2$ transition probabilities of the lowest bands in the groups $(++)$, $(+-)$, $(-+)$, and $(--)$ obtained by the 2DCH in comparison with the TAC [(a), (c), (e)] and the PRM [(b), (d), (f)].

arranged according to the energies, here we arrange the bands in the PRM based on energies as well, i.e., the lowest-energy states are defined as one band and the first excited-energy states as the partner band. In this way, the staggering feature is shown in the $B(M1)$ and $B(E2, I \rightarrow I - 1)$ values above $I = 15\hbar$.

Since we arrange the bands by energies as discussed above, it leads to the absence of staggering of the PRM values at spin $I = 19\hbar$ in Figs. 1(b), 1(d), and 1(f), and also the zero values of $B(E2, I \rightarrow I - 2)$ in Fig. 1(d) at low spin and at spin $I = 19\hbar$. These features can also be seen in Refs. [80,81].

At high spins ($I > 24\hbar$), the $B(M1)$ values in the 1DCH are different from those in the PRM. In particular, the $B(M1)$ values of the two bands in the PRM show remarkable differences for odd spins, while those in the 1DCH are similar. It should be noted that, in the PRM, there is a transition process from chiral rotation to principal axis rotation [82], and the two bands become no longer chiral partners at high spins. It is reflected by the increasing difference between the effective angle θ_{pn} of the two bands at high spins, as shown in Ref. [82]. The nonchiral quantum correlations induce remarkable differences for the $B(M1)$ values of the two bands. In the 1DCH, however, the semiclassical approximation is introduced and only the collective correlations in the azimuthal angle φ degree of freedom are considered. Therefore, the $B(M1)$ values of the two bands are similar.

B. Two-dimensional collective Hamiltonian

In Fig. 3, the intraband $M1$ and $E2$ transition probabilities of the lowest states in the groups $(++)$, $(+-)$, $(-+)$,

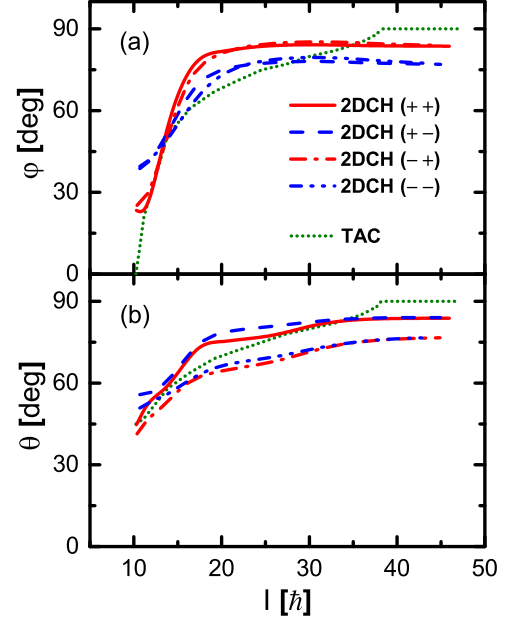


FIG. 4. The effective tilted cranking angles φ^{eff} and θ^{eff} of the lowest states in the groups $(++)$, $(+-)$, $(-+)$, and $(--)$ as functions of spin obtained by the 2DCH in comparison with the tilted cranking angles φ and θ by the TAC.

and $(--)$ obtained by the 2DCH are compared with those obtained by the TAC and the PRM.

In Figs. 3(a), 3(c), and 3(e), similar to the 1DCH, the tendencies of $M1$ and $E2$ transition probabilities of the yrast band (E_{++}^1) in the 2DCH agree well with those in the TAC. The $M1$ and $E2$ transition probabilities of the sidebands (E_{+-}^1 , E_{-+}^1 , E_{--}^1) and the yrast band are close to each other, as required by the chiral doublet bands or wobbling excitation bands.

In Fig. 3(a), the $B(M1)$ values in the 2DCH approach zero smoothly at high spin, differing from the case in the TAC. Same as in the 1DCH, this can be understood from the effective azimuthal angle φ^{eff} and polar angle θ^{eff} , respectively defined as

$$\varphi_{2\text{DCH}}^{\text{eff}} = \int_0^\pi d\theta \int_{-\pi/2}^{\pi/2} d\varphi \sqrt{w} |\varphi| |\Psi(\theta, \varphi)|^2, \quad (20)$$

$$\theta_{2\text{DCH}}^{\text{eff}} = \int_0^\pi d\theta \int_{-\pi/2}^{\pi/2} d\varphi \sqrt{w} (\pi/2 - |\pi/2 - \theta|) |\Psi(\theta, \varphi)|^2, \quad (21)$$

which are presented in Fig. 4.

At low spin ($I \leq 10\hbar$), the azimuth angle φ in the TAC is zero and the tilted cranking axis lies in the principal plane defined by the short and long axes, i.e., the so-called *planar solution* [2]. However, in the 2DCH, the effective azimuth angles φ^{eff} are not zero, due to the quantum fluctuation effects of the orientational axis. Such quantum effects correspond to the *chiral vibrations* in the low-spin region.

With increasing spin, the orientational axis does not lie in any of the principal planes in both the TAC and 2DCH. These are the so-called *aplanar solutions* [2], and they correspond to

the *chiral rotation*. The values of θ^{eff} and φ^{eff} in the 2DCH are close to but differ from θ and φ in the TAC due to the quantum fluctuations in both the φ and θ degrees of freedom.

At high spin ($I \geq 37\hbar$), the tilted cranking axis in the TAC is along the intermediate axis. As a consequence, the $B(M1)$ value in the TAC drops to zero. However, in the 2DCH, the effective angles ($\theta^{\text{eff}}, \varphi^{\text{eff}}$) do not equal $(\pi/2, \pi/2)$. Instead, the orientational axis has quantum fluctuations around the intermediate axis; corresponding to wobbling motions along θ and φ directions; namely, θ wobbling and φ wobbling [1]. Therefore, as in the 1DCH, the $B(M1)$ values in the 2DCH are nonvanishing at high spin due to the quantum effects.

One remarkable feature in Fig. 4 is that the effective angles φ^{eff} in the yrast band E_{++}^1 and the sideband E_{-+}^1 are close to each other, whereas θ^{eff} in the yrast band E_{++}^1 and the sideband E_{-+}^1 are close to each other. Similarly, φ^{eff} in bands E_{+-}^1 and E_{--}^1 are close to each other, and θ^{eff} in bands E_{+-}^1 and E_{--}^1 are close to each other. This is because the states E_{-+}^1 and E_{+-}^1 are one-phonon vibrational states with θ respectively based on the states E_{++}^1 and E_{+-}^1 . Similarly the states E_{+-}^1 and E_{--}^1 are the one-phonon states with φ respectively based on the states E_{++}^1 and E_{+-}^1 . The $(\theta^{\text{eff}}, \varphi^{\text{eff}})$ values for the yrast band (E_{++}^1) are almost the same as those for the sidebands ($E_{+-}^1, E_{-+}^1, E_{--}^1$) around the spin $I = 15\hbar$ in the 2DCH, which might be regarded as a signal for the static chirality in the 2DCH.

In Figs. 3(b), 3(d), and 3(f), the intraband $M1$ and $E2$ transition probabilities in the 2DCH are compared with those in the PRM. Again, the staggering behavior as well as the remarkable differences of $B(M1)$ values between the two bands at high spins in the PRM cannot be reproduced in the 2DCH. This is because the angular momentum in the 2DCH is not a good quantum number and only the collective correlations in the azimuthal angle φ and polar angle θ degrees of freedom are considered. Except for the staggering behavior, the amplitudes and tendencies of the $B(M1)$ and $B(E2)$ values in the PRM are reasonably reproduced by the 2DCH.

V. SUMMARY

In summary, the intraband EM transition probabilities are calculated in the framework of a collective Hamiltonian for chiral and wobbling modes. The EM transition probabilities for a system with one $h_{11/2}$ proton particle and one $h_{11/2}$ neutron hole coupled to a triaxial rotor ($\gamma = -30^\circ$) in the 1DCH and 2DCH are obtained and compared with the results given by the TAC and PRM.

The obtained EM transition probabilities for the yrast band and sidebands in the 1DCH and 2DCH are close to those in the TAC. At high spin, the $B(M1)$ transition probabilities in the 1DCH and 2DCH have nonvanishing values, as reflected by the effective orientational angles. This indicates that the missing quantum fluctuation effects of orientational axis are resumed.

The amplitudes and tendencies of the EM transition probabilities for the yrast and sidebands obtained in the PRM can be well reproduced by the 1DCH and 2DCH. However, the odd-even staggering of the $B(M1)$ values cannot be reproduced because the angular momentum is not a good quantum number in the 1DCH and 2DCH.

Based on the descriptions of the intraband EM transitions here and of the energy spectra in previous work [1], it will be interesting to build a collective Hamiltonian based on the microscopic tilted axis cranking covariant density-functional theory [47] for chiral and wobbling modes.

ACKNOWLEDGMENTS

X.H.W. thanks Fangqi Chen for helpful discussions. This work was partly supported by the National Key R&D Program of China (Contract No. 2018YFA0404400), the Deutsche Forschungsgemeinschaft (DFG), and the National Natural Science Foundation of China (NSFC) through funds provided to the Sino-German CRC 110 ‘‘Symmetries and the Emergence of Structure in QCD,’’ and the NSFC under Grants No. 11335002, No. 11621131001, and No. 11875075.

-
- [1] Q. B. Chen, S. Q. Zhang, P. W. Zhao, R. V. Jolos, and J. Meng, *Phys. Rev. C* **94**, 044301 (2016).
- [2] S. Frauendorf and J. Meng, *Nucl. Phys. A* **617**, 131 (1997).
- [3] A. Bohr and B. R. Mottelson, *Nuclear Structure*, Vol. II (Benjamin, New York, 1975).
- [4] J. Meng and S. Q. Zhang, *J. Phys. G* **37**, 064025 (2010).
- [5] J. Meng, Q. B. Chen, and S. Q. Zhang, *Int. J. Mod. Phys. E* **23**, 1430016 (2014).
- [6] R. A. Bark, E. O. Lieder, R. M. Lieder, E. A. Lawrie, J. J. Lawrie, S. P. Bvumbi, N. Y. Kheswa, S. S. Ntshangase, T. E. Madiba, P. L. Masiteng *et al.*, *Int. J. Mod. Phys. E* **23**, 1461001 (2014).
- [7] J. Meng and P. W. Zhao, *Phys. Scr.* **91**, 053008 (2016).
- [8] A. A. Raduta, *Prog. Part. Nucl. Phys.* **90**, 241 (2016).
- [9] S. Frauendorf, *Phys. Scr.* **93**, 043003 (2018).
- [10] B. W. Xiong and Y. Y. Wang, *At. Data Nucl. Data Tables* **125**, 193 (2019).
- [11] S. W. Ødegård, G. B. Hagemann, D. R. Jensen, M. Bergström, B. Herskind, G. Sletten, S. Törmänen, J. N. Wilson, P. O. Tjøm, I. Hamamoto *et al.*, *Phys. Rev. Lett.* **86**, 5866 (2001).
- [12] D. R. Jensen, G. B. Hagemann, I. Hamamoto, S. W. Ødegård, B. Herskind, G. Sletten, J. N. Wilson, K. Spohr, H. Hübel, P. Bringel *et al.*, *Phys. Rev. Lett.* **89**, 142503 (2002).
- [13] H. Amro, W. C. Ma, G. B. Hagemann, R. M. Diamond, J. Domscheit, P. Fallon, A. Görgen, B. Herskind, H. Höbel, D. R. Jensen *et al.*, *Phys. Lett. B* **553**, 197 (2003).
- [14] G. Schönwasser, H. Hübel, G. B. Hagemann, P. Bednarczyk, G. Benzoni, A. Bracco, P. Bringel, R. Chapman, D. Curien, J. Domscheit *et al.*, *Phys. Lett. B* **552**, 9 (2003).

- [15] P. Bringel, G. B. Hagemann, H. Hübel, A. Al-khatib, P. Bednarczyk, A. Bürger, D. Curien, G. Gangopadhyay, B. Herskind, D. R. Jensen *et al.*, *Eur. Phys. J. A* **24**, 167 (2005).
- [16] D. J. Hartley, R. V. F. Janssens, L. L. Riedinger, M. A. Riley, A. Aguilar, M. P. Carpenter, C. J. Chiara, P. Chowdhury, I. G. Darby, U. Garg *et al.*, *Phys. Rev. C* **80**, 041304(R) (2009).
- [17] J. T. Matta, U. Garg, W. Li, S. Frauendorf, A. D. Ayangeakaa, D. Patel, K. W. Schlax, R. Palit, S. Saha, J. Sethi *et al.*, *Phys. Rev. Lett.* **114**, 082501 (2015).
- [18] S. Biswas, R. Palit, S. Frauendorf, U. Garg, W. Li, G. H. Bhat, J. A. Sheikh, J. Sethi, S. Saha, P. Singh *et al.*, [arXiv:1608.07840](https://arxiv.org/abs/1608.07840).
- [19] S. J. Zhu, Y. X. Luo, J. H. Hamilton, A. V. Ramayya, X. L. Che, Z. Jiang, J. K. Hwang, J. L. Wood, M. A. Stoyer, R. Donangelo *et al.*, *Int. J. Mod. Phys. E* **18**, 1717 (2009).
- [20] Y. X. Luo, J. H. Hamilton, A. V. Ramayya, J. K. Hwang, S. H. Liu, J. O. Rasmussen, S. Frauendorf, G. M. Ter-Akopian, A. V. Daniel, and Y. T. Oganessian, in *Proceedings of the International Symposium, Vladivostok, Russia*, edited by Yu E. Penionzhkevich and Yu G. Sobolev (World Scientific, Singapore, 2012).
- [21] J. Peng, J. Meng, and S. Q. Zhang, *Phys. Rev. C* **68**, 044324 (2003).
- [22] T. Koike, K. Starosta, and I. Hamamoto, *Phys. Rev. Lett.* **93**, 172502 (2004).
- [23] K. Tanabe and K. Sugawara-Tanabe, *Phys. Rev. C* **73**, 034305 (2006).
- [24] S. Q. Zhang, B. Qi, S. Y. Wang, and J. Meng, *Phys. Rev. C* **75**, 044307 (2007).
- [25] K. Higashiyama and N. Yoshinaga, *Eur. Phys. J. A* **33**, 355 (2007).
- [26] K. Tanabe and K. Sugawara-Tanabe, *Phys. Rev. C* **77**, 064318 (2008).
- [27] B. Qi, S. Q. Zhang, J. Meng, S. Y. Wang, and S. Frauendorf, *Phys. Lett. B* **675**, 175 (2009).
- [28] Q. B. Chen, J. M. Yao, S. Q. Zhang, and B. Qi, *Phys. Rev. C* **82**, 067302 (2010).
- [29] E. A. Lawrie and O. Shirinda, *Phys. Lett. B* **689**, 66 (2010).
- [30] S. G. Rohoziński, L. Próchniak, K. Starosta, and C. Droste, *Eur. Phys. J. A* **47**, 90 (2011).
- [31] O. Shirinda and E. A. Lawrie, *Eur. Phys. J. A* **48**, 118 (2012).
- [32] H. Zhang and Q. B. Chen, *Chin. Phys. C* **40**, 024102 (2016).
- [33] I. Hamamoto, *Phys. Rev. C* **65**, 044305 (2002).
- [34] I. Hamamoto and B. R. Mottelson, *Phys. Rev. C* **68**, 034312 (2003).
- [35] S. Frauendorf and F. Dönau, *Phys. Rev. C* **89**, 014322 (2014).
- [36] W. X. Shi and Q. B. Chen, *Chin. Phys. C* **39**, 054105 (2015).
- [37] K. Tanabe and K. Sugawara-Tanabe, *Phys. Rev. C* **95**, 064315 (2017).
- [38] R. Budaca, *Phys. Rev. C* **97**, 024302 (2018).
- [39] Q. B. Chen, K. Starosta, and T. Koike, *Phys. Rev. C* **97**, 041303(R) (2018).
- [40] Q. B. Chen, B. F. Lv, C. M. Petrache, and J. Meng, *Phys. Lett. B* **782**, 744 (2018).
- [41] E. Streck, Q. B. Chen, N. Kaiser, and U.-G. Meißner, *Phys. Rev. C* **98**, 044314 (2018).
- [42] R. Budaca, *Phys. Rev. C* **98**, 014303 (2018).
- [43] V. I. Dimitrov, S. Frauendorf, and F. Dönau, *Phys. Rev. Lett.* **84**, 5732 (2000).
- [44] P. Olbratowski, J. Dobaczewski, J. Dudek, and W. Płóciennik, *Phys. Rev. Lett.* **93**, 052501 (2004).
- [45] P. Olbratowski, J. Dobaczewski, and J. Dudek, *Phys. Rev. C* **73**, 054308 (2006).
- [46] I. Kuti, Q. B. Chen, J. Timár, D. Sohler, S. Q. Zhang, Z. H. Zhang, P. W. Zhao, J. Meng, K. Starosta, T. Koike *et al.*, *Phys. Rev. Lett.* **113**, 032501 (2014).
- [47] P. W. Zhao, *Phys. Lett. B* **773**, 1 (2017).
- [48] C. M. Petrache, B. F. Lv, A. Astier, E. Dupont, Y. K. Wang, S. Q. Zhang, P. W. Zhao, Z. X. Ren, J. Meng, P. T. Greenlees *et al.*, *Phys. Rev. C* **97**, 041304(R) (2018).
- [49] H. G. Ganev, A. I. Georgieva, S. Brant, and A. Ventura, *Phys. Rev. C* **79**, 044322 (2009).
- [50] S. Brant, D. Vretenar, and A. Ventura, *Phys. Rev. C* **69**, 017304 (2004).
- [51] A. A. Raduta, C. M. Raduta, and A. Faessler, *J. Phys. G* **41**, 035105 (2014).
- [52] A. A. Raduta, A. H. Raduta, and C. M. Petrache, *J. Phys. G* **43**, 095107 (2016).
- [53] K. Higashiyama, N. Yoshinaga, and K. Tanabe, *Phys. Rev. C* **72**, 024315 (2005).
- [54] G. H. Bhat, J. A. Sheikh, W. A. Dar, S. Jehangir, R. Palit, and P. A. Ganai, *Phys. Lett. B* **738**, 218 (2014).
- [55] F. Q. Chen, Q. B. Chen, Y. A. Luo, J. Meng, and S. Q. Zhang, *Phys. Rev. C* **96**, 051303(R) (2017).
- [56] M. Shimada, Y. Fujioka, S. Tagami, and Y. R. Shimizu, *Phys. Rev. C* **97**, 024318 (2018).
- [57] M. Shimada, Y. Fujioka, S. Tagami, and Y. R. Shimizu, *Phys. Rev. C* **97**, 024319 (2018).
- [58] F. Q. Chen, J. Meng, and S. Q. Zhang, *Phys. Lett. B* **785**, 211 (2018).
- [59] S. Mukhopadhyay, D. Almeded, U. Garg, S. Frauendorf, T. Li, P. V. M. Rao, X. Wang, S. S. Ghugre, M. P. Carpenter, S. Gros *et al.*, *Phys. Rev. Lett.* **99**, 172501 (2007).
- [60] D. Almeded, F. Dönau, and S. Frauendorf, *Phys. Rev. C* **83**, 054308 (2011).
- [61] Y. R. Shimizu and M. Matsuzaki, *Nucl. Phys. A* **588**, 559 (1995).
- [62] M. Matsuzaki, Y. R. Shimizu, and K. Matsuyanagi, *Phys. Rev. C* **65**, 041303(R) (2002).
- [63] M. Matsuzaki, Y. R. Shimizu, and K. Matsuyanagi, *Eur. Phys. J. A* **20**, 189 (2004).
- [64] M. Matsuzaki, Y. R. Shimizu, and K. Matsuyanagi, *Phys. Rev. C* **69**, 034325 (2004).
- [65] M. Matsuzaki and S.-I. Ohtsubo, *Phys. Rev. C* **69**, 064317 (2004).
- [66] Y. R. Shimizu, M. Matsuzaki, and K. Matsuyanagi, *Phys. Rev. C* **72**, 014306 (2005).
- [67] Y. R. Shimizu, T. Shoji, and M. Matsuzaki, *Phys. Rev. C* **77**, 024319 (2008).
- [68] T. Shoji and Y. R. Shimizu, *Prog. Theor. Phys.* **121**, 319 (2009).
- [69] S. Frauendorf and F. Dönau, *Phys. Rev. C* **92**, 064306 (2015).
- [70] Q. B. Chen, S. Q. Zhang, P. W. Zhao, R. V. Jolos, and J. Meng, *Phys. Rev. C* **87**, 024314 (2013).
- [71] Q. B. Chen, S. Q. Zhang, P. W. Zhao, and J. Meng, *Phys. Rev. C* **90**, 044306 (2014).
- [72] Q. B. Chen, S. Q. Zhang, and J. Meng, *Phys. Rev. C* **94**, 054308 (2016).
- [73] S. Y. Wang, S. Q. Zhang, B. Qi, and J. Meng, *Chin. Phys. Lett.* **24**, 664 (2007).
- [74] P. Ring and P. Schuck, *The Nuclear Many-Body Problem* (Springer-Verlag, Berlin, 1980).
- [75] M. Baranger and K. Kumar, *Nucl. Phys. A* **122**, 241 (1968).

- [76] M. Matsuo, T. Nakatsukasa, and K. Matsuyanagi, *Prog. Theor. Phys.* **103**, 959 (2000).
- [77] K. Matsuyanagi, M. Matsuo, T. Nakatsukasa, N. Hinohara, and K. Sato, *J. Phys. G* **37**, 064018 (2010).
- [78] W. Pauli, *Handbuch der Physik* (Springer-Verlag, Berlin, 1933).
- [79] S. Frauendorf, *Nucl. Phys. A* **677**, 115 (2000).
- [80] B. Qi, J. Meng, S.-Q. Zhang, S.-Y. Wang, and J. Peng, *Chin. Phys. C* **33**, 43 (2009).
- [81] B. Qi, S. Q. Zhang, S. Y. Wang, J. M. Yao, and J. Meng, *Phys. Rev. C* **79**, 041302(R) (2009).
- [82] Q. B. Chen and J. Meng, *Phys. Rev. C* **98**, 031303(R) (2018).